ACS Catalysis

Research Article

pubs.acs.org/acscatalysis

Selectivity and Reactivity of Alkylamine- and Alkanethiolate-Stabilized Pd and PdAg Nanoparticles for Hydrogenation and Isomerization of Allyl Alcohol

Monica Moreno,[†] Lyndsay N. Kissell,[†] Jacek B. Jasinski,[‡] and Francis P. Zamborini*[,†]

[†]Department of Chemistry and [‡]Conn Center for Renewable Energy Research, University of Louisville, Louisville, Kentucky 40292, United States

Supporting Information

ABSTRACT: Here, we describe the stability of solutions of various Pd and PdAg organic-protected nanoparticles (NPs) in the presence of H_2 and their selectivity and reactivity as catalysts for hydrogenation or isomerization of allyl alcohol. Pd and $Pd_{91}Ag_9$ NPs stabilized with hexadecylamine ($C16NH_2$) ligands are stable against H_2-induced aggregation, whereas those stabilized with octylamines ($C8NH_2$) and dodecylamines ($C12NH_2$) precipitate within 1 h. The stability of $C16NH_2$ Pd NPs is comparable to that of hexanethiolate (C6S)-protected Pd NPs and mixed monolayer C6S/$C8NH_2$ (1/1) Pd NPs that were studied previously. The stability of $C16NH_2$ Pd NPs decreases as the alkylamine/Pd^{II} ratio used in the synthesis decreases from 12:1 to 6:1 to 3:1. A bilayer or partial bilayer of $C16NH_2$ ligands forms around the Pd core for ratios greater than 6:1, which explains the higher stability of these NPs against aggregation. The various Pd and PdAg NPs catalyzed the hydrogenation and isomerization of allyl alcohol in the presence of H_2 with various selectivities and reactivities. C6S Pd NP catalysts are >95% selective toward the isomer; $C8NH_2$/C6S Pd NPs are 60−75% selective toward the isomer, depending on the ligand ratio; and $CnNH_2$-coated Pd NPs generally produce a 1:1 or 3:2 ratio of the hydrogenation/isomerization products, with a few exceptions. The catalytic turnover frequency (TOF) is low for C6S Pd NPs becaue of the strong thiolate−Pd bond. The TOF increases with increasing chain length in the order $C16NH_2$ Pd > $C12NH_2$ Pd > $C8NH_2$ Pd and increases for $Pd_{91}Ag_9$ alloys compared with pure Pd. The mixed ligand $C8NH_2$/C6S Pd NPs exhibit TOFs similar to pure $C8NH_2$ Pd for low thiol content and similar to C6S Pd NPs for high thiol content. The 130/150 $C8NH_2$/C6S Pd exhibits the optimal TOF for the mixed monolayer Pd NPs. $C16NH_2$ $Pd_{91}Ag_9$ has the highest TOF of all the NPs studied due to the high stability afforded by the bilayer structure of the C16 chain and the high reactivity due to very little interference from the weak metal−amine interaction. Several of the Pd NPs that are stable in the presence of H_2 are not stable during the catalysis reaction (H_2 plus allyl alcohol), showing that the substrate also plays a role in NP stability.

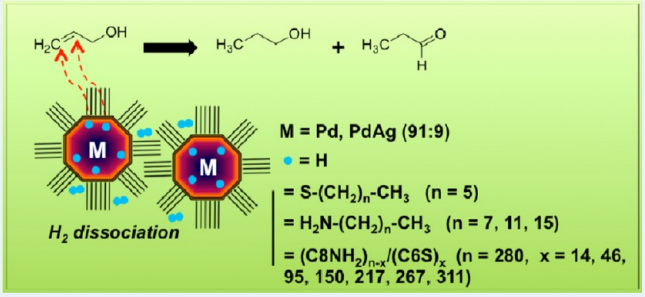

KEYWORDS: *palladium, nanoparticles, catalysis, allyl alcohol, hydrogenation, isomerization*

INTRODUCTION

Research on metal nanoparticles (NPs) has been highly active in recent years as a result of their unique, size-tunable properties, which are different from the bulk materials.[1,2] In particular, their high surface-to-volume ratio and size-dependent electronic structure have made metal NPs attractive materials for many applications, including sensing,[3−6] imaging,[7] drug delivery,[8,9] cancer diagnosis and therapy,[10,11] hydrogen storage,[12−14] and catalysis.[15−19] A key issue for the application of these materials in catalysis is control of the size, shape, composition, and stability of the NPs,[20−25] which can be accomplished through synthesis and functionalization of the NPs with organic stabilizers, such as polymers,[26−29] dendrimers,[23,30−33] surfactants,[34−36] or ligands.[37−43] A major challenge is to sufficiently protect the NP against irreversible aggregation or major morphology changes under the conditions of the reaction being catalyzed while retaining high catalytic activity on the NP surface.[27]

Several strategies have been reported for homogeneous catalysis with metallic nanostructures.[20] Here, we review those that focus on Pd NPs, since this is the subject of our work. Crooks and co-workers reported the use of Pd NPs encapsulated in dendrimers for catalyzing the hydrogenation of unsaturated organic compounds[44,45] and C−C coupling reactions such as Heck[46] and Stille[47] reactions. They studied the effect of NP size on hydrogenation reactions[44] and also developed a fluorous phase Pd−dendrimer catalyst that could be recycled and reused numerous times.[48] The benefit of dendrimers is that they stabilize the NPs but allow molecules to

Received: June 8, 2012
Revised: September 14, 2012
Published: October 22, 2012

access the NP surface for catalysis, and they can impart some selectivity into the reaction. El-Sayed and co-workers directly compared the catalytic activity and stability of polyvinylpyrrolidone (PVP)-stabilized Pd NPs in solution to PVP−Pd NPs adsorbed onto carbon for catalyzing the Suzuki coupling reaction.[49] They observed that although the carbon-supported Pd NPs were less catalytically active, they were highly recyclable, making them potentially better catalysts for the Suzuki reaction compared with colloidal Pd NPs. Sastry and co-workers synthesized Pt and Pd NPs immobilized on the surface of amine-functionalized zeolite.[50] They found that the rate of hydrogenation and Heck reactions over these catalysts was much higher than those obtained using conventionally prepared catalysts.[50]

Although the majority of studies have been conducted using supported metal NPs as catalysts for a variety of organic and inorganic reactions, these heterogeneous systems suffer from low catalytic rates, limited lifetime, complex methods of preparation, and poor particle morphology control.[49,50] Most of the homogeneous Pd catalysts described in the literature are stabilized with polymers (including dendrimers) or surfactants.[17,20] They are used because of the fairly weak affinity to the metal NP, enabling catalytic activity and stability. They have some disadvantages, however. It has been demonstrated that metal NPs in solution are unstable and undergo changes in their morphology in the reaction mixture. In addition, the colloidal NPs are often not stable in solvent-free form, making separation, recovery, and regeneration of the catalyst difficult.[17,49−51] Clearly, there is still a need to synthesize highly stable and reactive NPs with high recyclability for applications in homogeneous catalysis.

In 1994, Brust and co-workers reported, for the first time, an easy and reproducible synthesis for the preparation of Au NPs stabilized with self-assembled monolayers of dodecanethiolate ligands.[52] These roughly spherical particles have a core of metallic atoms surrounded by an organic monolayer. Alkanethiolate-protected Au NPs are highly stable, can be stored as solids, are easily characterized, and are easily separated from reaction products.[39] Au, Pd, and Pt NPs stabilized with thiols have drawn popular research interest;[5,37−41,53−56] however, they have not been widely used in the catalysis field because the stabilizing ligand is usually strongly bound to the metal core, and therefore, the catalytic activity is greatly inhibited.[29,38,43,57]

A few reports have described the synthesis and catalytic activity of Pt NPs protected by a thiol monolayer in hydrogenation reactions[40,43] and their electrocatalytic properties in methanol oxidation.[37,41] Pd NPs coated with *n*-alkylamines have also been used for the electrochemical oxidation of methane.[42] Astruc and co-workers investigated for the first time the catalytic properties of Pd−dodecanethiolate NPs in the Suzuki−Miyaura C−C coupling reaction of aromatic iodides and bromides under ambient conditions.[38] These catalysts showed modest yields, but they were phosphine-free and recyclable. Later, Fornasiero and co-workers reported a convenient approach for the preparation of Pd NPs coated with thiols and their easy recycling/reuse in the Suzuki cross-coupling reaction.[55] Recently, Shon and co-workers showed that alkanethiolate-coated Pd and PdAu NPs selectively catalyze the isomerization of allyl alcohol over the hydrogenation.[58,59]

Catalytic selective hydrogenation of allyl alcohol to produce 1-propanol, which is a precursor in organic synthesis and the pharmaceutical industry, has been studied as a function of the particle size and shape of Pd NPs coated with polymers,[60,61] biopolymers (collagen fiber),[62] surfactants,[34] or dendrimers[30,31,33,44,45,63,64] either in solution or immobilized on solid supports such as alumina,[34,60] composites,[33] silica,[65] and magnetic NP cores.[66−68] However, the transformation of allyl alcohol to carbonyl compounds (isomerization reaction) has not been widely explored using Pd NPs as catalysts. The isomerization reaction is an important and useful synthetic process because it leads to the formation of carbonyl compounds in a one-pot catalytic transformation, avoiding the two-step sequential oxidation and reduction reactions (Scheme 1).[69,70] In particular, the isomerization of allyl alcohol

Scheme 1. Transformation of Allyl Alcohols into Saturated Carbonyl Compounds

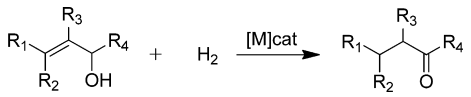

is an attractive strategy that offers environmental and economical advantages because no byproducts are generated; therefore, only the corresponding saturated aldehydes or ketones are obtained, which are valuable and versatile synthetic intermediates for various pharmaceuticals, agrochemicals, and fine chemicals.[69−72] There are two main mechanisms proposed for this reaction, in which migration of the double bond leads to formation of an enol intermediate that tautomerizes to a saturated carbonyl compound irreversibly.[70,71] In many cases, the isomerization reaction requires relatively high quantities of catalyst, harsh reaction conditions, and expensive metals.[72] Although several transition metals have been used to perform this reaction, ruthenium, rhodium, and iron have shown the best selectivity and activity.[70,71,73,74]

Pietropaolo and co-workers reported the catalytic hydrogenation and isomerization of allyl alcohols over supported Pd catalysts.[75] They found that the reaction between α,β-unsaturated alcohols and H_2 over Pd/TiO_2 catalysts exhibited high activity and selectivity for the double bond migration, leading to a high yield of the corresponding saturated aldehyde or ketones.[75] Zharmagambetova and co-workers studied the route of the catalytic reaction of allyl alcohol with hydrogen on polymer−Pd(0) and −Pd(II) complexes.[76] They determined that catalytic activity and selectivity depend on the Pd valence state, structure of the polymer matrix, and functional groups.[76] To our knowledge, there is only one report regarding the utilization of alkanethiolate-capped Pd MPCs as homogeneous catalysts for the isomerization of allyl alcohols.[58] Shon and co-workers showed the isomerization of allyl alcohol to the corresponding carbonyl compound with a relatively high selectivity (95%) compared with other Pd-based catalysts (<75%).[58,59]

In our previous work, we described the reactivity between hydrogen and solutions and films of Pd NPs coated with pure hexanethiolate (C6S), octylamine ($C8NH_2$), dodecylamine ($C12NH_2$), hexadecylamine ($C16NH_2$), and mixed $C8NH_2$/C6S ligands as well as PdAg (10:1) and PdAu (10:1) alloy NPs stabilized with C6S, $C8NH_2$, and $C12NH_2$.[57,77,78] The reactivity with H_2 and stability against morphology changes could be controlled by changing the metal and organic monolayer composition on the NP surface. These studies focused mainly on the reactivity for H_2 sensing applications.

dx.doi.org/10.1021/cs300361y | *ACS Catal.* 2012, 2, 2602−2613

Here, we describe catalysis applications of these materials in which H_2 gas is one of the reactants. We compare the catalytic activity of various alkylamine, alkanethiolate, and mixed ligand Pd and PdAg NPs for hydrogenation and isomerization of 2-propen-1-ol in the presence of H_2. Although Shon recently showed highly selective isomerization with alkanethiolate-coated Pd NPs, this report is the first to directly compare alkanethiolate-, alkylamine-, and mixed ligand organic-protected Pd and PdAg NPs for the hydrogenation and isomerization of allyl alcohol.

EXPERIMENTAL SECTION

Chemicals. Toluene (99.9%), 2-propanol (99.9%), acetone (99%), acetonitrile (99%), dichloromethane (99.5%), and ethanol (200 proof) were purchased from VWR Scientific Products and used as received. Hexanethiol (95%), dodecylamine (98%), sodium borohydride (98%), potassium tetrachloropalladate(II) (98%), silver trifluoroacetate (98%), allyl alcohol (99%), propionaldehyde (99%), propyl alcohol (99.7%), and chloroform-*d* (99.8%) were purchased from Aldrich Chemical Co. and used as received. Tetraoctylammonium bromide (98%), octylamine (99%), and 1-hexadecylamine (90%) containing 1-octadecylamine were purchased from Alfa Aesar Co. and used as received. Barnstead nanopure water (18.3 MΩ cm) was employed for all aqueous solutions.

Synthesis of Hexanethiolate-Coated Pd NPs (C6S Pd NPs). Hexanethiolate-coated (C6S) Pd NPs were synthesized as reported previously.[39,57,77,78] Briefly, 0.50 g of K_2PdCl_4 in 10 mL of water was transferred into the toluene phase (100 mL) using 1.25 g of TOABr as indicated by the colorless toluene layer becoming deep red (~30 min). The colorless water layer was removed, and 110 μL of hexanethiol was added to the toluene solution in a 1:2 hexanethiol/Pd ratio. The solution was cooled in an ice bath for 45 min, and 0.60 g of $NaBH_4$ in 10 mL of water was added with stirring. The solution was removed from the ice bath after 10 min and stirred for 4 h at room temperature. The water layer was discarded, and the toluene was removed by rotary evaporation. The black Pd NP product was suspended in 200 mL of acetonitrile overnight and collected by vacuum filtration on a glass-fritted Büchner funnel. The NPs were washed with acetonitrile and ethanol successively two times before thoroughly drying and collecting. These NPs are referred to as 1/2x C6S Pd NPs.

Synthesis of Alkylamine-Coated Pd and PdAg NPs ($CnNH_2$ Pd and $CnNH_2$ PdAg NPs). Alkylamine-coated Pd NPs were synthesized at room temperature according to our previous reports.[77,78] Solutions of 0.50 g (1.53 mmol) of K_2PdCl_4 in 10 mL of water and 1.67 g (3.06 mmol) of TOABr in 70 mL of toluene were combined and stirred until all $PdCl_4^{2-}$ transferred into the toluene phase, then the appropriate alkylamine ligand was added in a 12:1 alkylamine/Pd ratio, and the solution was rapidly stirred for 45 min. This ratio corresponds to 18.4 mmol of alkylamine, which is 2.97 mL for octylamine ($C8NH_2$), 3.34 g for dodecylamine ($C12NH_2$), and 4.35 g for 1-hexadecylamine ($C16NH_2$). These syntheses are referred to as 12x $C8NH_2$ Pd, 12x $C12NH_2$ Pd, and 12x $C16NH_2$ Pd. The organic layer became light yellow, whereas the aqueous layer turned cloudy white upon addition of the alkylamine. This could be due to complexation between the protonated amine and $PdCl_4^{2-}$, but it is not certain, since this precipitate has not been characterized.[79] Next, 0.87 g of $NaBH_4$ (23.0 mmol) in 10 mL of water was added to the two-phase solution while stirring. The organic phase quickly turned black, and the cloudiness in the aqueous phase disappeared after about 2 min. The solution was stirred for 3 h, the clear and colorless water layer was separated, and the toluene layer was later removed by evaporation. The black Pd NP product was suspended in 100 mL of acetonitrile overnight and collected by vacuum filtration. The resulting NPs were washed with acetonitrile and ethanol to remove excess ligands and other reaction byproducts before collecting. For 12x $C12NH_2$ Pd and 12x $C16NH_2$ Pd NPs, the solid was redissolved in toluene, and the solvent was reduced in volume by rotary evaporation. The black NPs were precipitated in acetone overnight, and the precipitate was collected by vacuum filtration before washing with acetone and ethanol. Two other samples with $C16NH_2$/Pd of 6:1 (6x) and 3:1 (3x) were also synthesized. The five $CnNH_2$ Pd NPs were black powders and soluble in nonpolar solvents.

Alkylamine-coated PdAg NPs were synthesized by adding the appropriate amount of K_2PdCl_4 and $AgC_2F_3O_2$ salts in a 10:1 ratio.[77] $AgC_2F_3O_2$ was directly soluble in the toluene phase, whereas $PdCl_4^{2-}$ was phase-transferred into toluene with TOABr. The amount of $C8NH_2$, $C12NH_2$, and $C16NH_2$ was 12:1 with respect to the total metal content. These syntheses are referred to as 12x $C8NH_2$, 12x $C12NH_2$, and 12x $C16NH_2$ PdAg NPs. A 15-fold excess of $NaBH_4$ with respect to total metal (Pd and Ag) was added to the solution. PdAg NPs were cleaned in the same way as the corresponding Pd NPs.

Synthesis of Pd NPs Coated with Mixed Octylamine and Hexanethiolate Ligands ($C8NH_2$/C6S Pd NPs). The synthesis of Pd NPs coated with a mixture of $C8NH_2$ and C6S ligands was performed by a ligand place-exchange reaction, in which ~0.015 g of $C8NH_2$ Pd NPs was dissolved in 5.0 mL of CH_2Cl_2 before addition of a variable amount of C6SH (0.1 to 3 μL), as reported previously.[78] The solution was stirred for 30−45 min and then used for stability and catalysis studies. We previously confirmed by NMR that the C6S ligands fully replace the $C8NH_2$ ligands on the Pd NPs. Since we did not purify the sample, there should have been free $C8NH_2$ ligands in solution that were removed from the Pd NPs by the C6S ligands. The free $C8NH_2$ ligands were not removed from the solution since they did not significantly affect the stability and catalysis results.

Characterization. Transmission electron microscopy (TEM) images of Pd and PdAg NPs were recorded at different magnifications using a FEI Tecani F20 field-emission (FE) TEM operating at an accelerating voltage of 200 keV. Samples were prepared by casting a single drop of a dilute toluene solution of Pd and PdAg NPs onto a copper grid-supported holey carbon film and allowing the solvent to evaporate. Particle sizes were determined manually from digital images. Energy dispersive X-ray (EDX) analysis of Pd and PdAg NPs was performed using an EDX spectrometer in the FEI Tecani F20 FEI-TEM. These measurements were performed in the scanning TEM (STEM) mode using the nanoprobe configuration with a probe size down to about 1 nm. EDX combined with TEM provided the means to accurately identify the metal composition. Thermogravimetric analysis (TGA) of the NPs was obtained over a temperature range of 25−800 °C at a heating rate of 20 °C/min on a 2950 TGA HR V5.4A instrument under nitrogen using sample sizes of 17.1−20.8 mg.

Spectroscopic Measurements. The optical properties of alkylamine-coated Pd and PdAg NPs were evaluated over the range of 300−900 nm using a Varian Cary 50 Bio UV−visible spectrophotometer. At room temperature, two or three drops

dx.doi.org/10.1021/cs300361y | ACS Catal. 2012, 2, 2602−2613

of 10 mg/mL toluene solutions of Pd and PdAg NPs were placed in a 1 cm path length quartz cuvette and diluted further with toluene. The baseline of each spectrum was corrected using the spectrum of toluene. The absorbance spectrum of the solutions was measured following exposure to pure H_2 bubbling through the solution at a flow rate of 8.0 ± 0.2 mL/min for 0, 5, 15, 30, and 60 min. After exposing to H_2 for 60 min, the solutions were sonicated for 2 min and drop-cast-deposited onto a copper grid-supported holey carbon film for TEM measurements. ^{1}H NMR spectra were recorded on a 500 MHz INOVA spectrometer in $CDCl_3$ solutions internally referenced to $CDCl_3$ at δ 7.26 ppm. The NMR spectra confirmed the successful synthesis and purity of the Pd and PdAg NPs.

Catalysis Experiments. The catalysis experiments were performed by placing 3.5 mL of CH_2Cl_2 and 1.5 mmol of allyl alcohol (100 μL) in a small glass reaction vessel. The solution was stirred for 10 min before adding ~3.0 mg of Pd or PdAg NP catalyst. The vessel was capped with a rubber septum and H_2 gas was allowed to bubble through the solution at a flow rate of 8.0 ± 0.2 mL/min for the duration of the experiment. The total volume was kept constant by adding solvent to the vessel when evaporation occurred. The reaction mixture was stirred at 500−600 rpm under atmospheric pressure and at room temperature. The progress of the reaction was followed by gas chromatography of samples before exposure to H_2 and after addition of catalyst and exposure to H_2 for different times. Gas chromatography data were recorded on a Buck Scientific model 910 gas chromatograph equipped with a 1/8 in. packed column (10% carbowax 20 M on silica 80/100 mesh, 6 foot) using a flame ionization detector (FID) and helium as the carrier gas. The catalytic reaction was monitored using response factors that were determined with a standard mixture containing 10 mM of each reactant, product, and isomer as reported previously by Bruening.[80] The turnover frequency (TOF) was calculated from the slope of the linear portion (<60% conversion of reactant to isomer and hydrogenated product) of the plot of percent hydrogenation and percent isomerization versus time. The slopes were determined by forcing the intercept through zero. The TOF was calculated as the average of three samples analyzed for each catalyst with the standard deviation shown. The Supporting Information provides an example of the TOF calculation.[80] The progress of the catalytic reaction was also followed by ^{1}H NMR analysis (data not shown). Since the concentration of Pd and PdAg NPs was less than that of the substrates and the NMR peaks associated with their ligands were at different positions, they did not interfere with the NMR signal of the substrates.[40]

RESULTS AND DISCUSSION

Synthesis and Composition of Pd and PdAg NPs. Scheme 2 illustrates the various metal compositions (Pd and PdAg) and protecting ligands used in our previous work and in this study, which includes hexanethiolate (C6S), octylamine ($C8NH_2$), dodecylamine ($C12NH_2$), hexadecylamine ($C16NH_2$), and mixed $C8NH_2$/C6S.[77,78] Nuclear magnetic resonance (NMR), Fourier transform infrared (FTIR) spectroscopy, and UV−vis spectroscopy measurements on Pd and PdAg NPs were consistent with the successful synthesis of pure NPs.

The use of stabilizers with metal NPs plays a crucial role in controlling the particle size and shape and the catalytic activity of the NPs.[20,25] Table 1 shows the average diameter from TEM measurements, the organic weight percent from TGA, and the very roughly estimated compositions of Pd and PdAg NPs coated with different capping ligands. Figure S-1 of the Supporting Information presents TEM images of the various

Scheme 2. Illustration of the NPs with Different Metal Compositions and Different Ligand Stabilizers Used in This Study

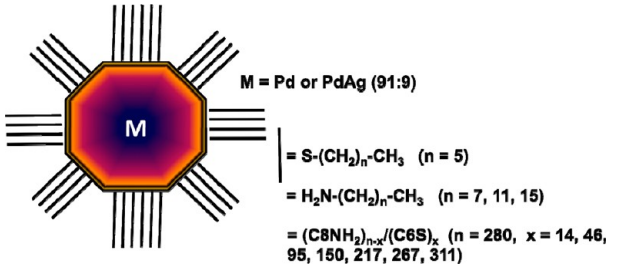

Table 1. Characterization and Composition of the Pd and PdAg NPs

nanoparticles[a]	TEM[b] diameter (nm)	TGA wt % organic	composition
1/2x C6S Pd#	3.4 ± 0.5	18.8	Pd_{1334} $(C6S)_{278}$
12x $C8NH_2$ Pd*	3.5 ± 0.4	18.9	Pd_{1455} $(C8NH_2)_{280}$
12x $C12NH_2$ Pd*	3.4 ± 0.6	22.0	Pd_{1334} $(C12NH_2)_{217}$
12x $C16NH_2$ Pd#	3.0 ± 0.5	83.6	Pd_{916} $(C16NH_2)_{2057}$
6x $C16NH_2$ Pd*	3.1 ± 0.4	57.9	Pd_{1011} $(C16NH_2)_{614}$
3x $C16NH_2$ Pd*	5.1 ± 1.0	14.4	Pd_{4502} $(C16NH_2)_{334}$
12x $C8NH_2$ $Pd_{91}Ag_9$*	2.8 ± 0.7	20.8	Pd_{672} Ag_{66} $(C8NH_2)_{161}$
12x $C12NH_2$ $Pd_{91}Ag_9$*	2.5 ± 0.3	17.8	Pd_{478} Ag_{47} $(C12NH_2)_{65}$
12x $C16NH_2$ $Pd_{91}Ag_9$#	2.9 ± 0.4	86.9	Pd_{746} Ag_{74} $(C16NH_2)_{2398}$
$C8NH_2$/C6S (266/14) Pd$^\perp$	3.5 ± 0.4		Pd_{1455} $(C8NH_2)_{266}$ $(C6S)_{14}$
$C8NH_2$/C6S (234/46) Pd$^\perp$	3.5 ± 0.4		Pd_{1455} $(C8NH_2)_{234}$ $(C6S)_{46}$
$C8NH_2$/C6S (185/95) Pd$^\perp$	3.5 ± 0.4		Pd_{1455} $(C8NH_2)_{185}$ $(C6S)_{95}$
$C8NH_2$/C6S (130/150) Pd$^\perp$	3.5 ± 0.4		Pd_{1455} $(C8NH_2)_{130}$ $(C6S)_{150}$
$C8NH_2$/C6S (63/217) Pd$^\perp$	3.5 ± 0.4		Pd_{1455} $(C8NH_2)_{63}$ $(C6S)_{217}$
$C8NH_2$/C6S (13/267) Pd$^\perp$	3.5 ± 0.4		Pd_{1455} $(C8NH_2)_{13}$ $(C6S)_{267}$
$C8NH_2$/C6S (0/311) Pd$^\perp$	3.5 ± 0.4		Pd_{1455} $(C8NH_2)_0$ $(C6S)_{311}$

[a]# = these NPs were stable and appeared as well-isolated, individual structures. * = these NPs showed several aggregated structures in the TEM images before any H_2 exposure and have the most uncertainty in the TEM measured diameter and overall composition. ⊥ = no TEM or TGA data was obtained. The diameter shown is that of the original $C8NH_2$ NPs and composition based on full replacement of $C8NH_2$ with C6S on the Pd NP. [b]The average particle sizes were obtained from counting only individual, well-isolated nanoparticles in the TEM images (see Figure S-1, Supporting Information). Larger, irregular shaped structures were not included because it was uncertain if those originally existed that way or became aggregated in solution or upon drying.

dx.doi.org/10.1021/cs300361y | ACS Catal. 2012, 2, 2602−2613

NPs on carbon-coated copper grids. The average diameter of the 1/2x C6S Pd NPs was 3.4 nm, similar to the core diameter previously reported for alkanethiolate-protected Pd NPs.[39,57] The average diameter of 12x $C8NH_2$, 12x $C12NH_2$, and 12x $C16NH_2$ Pd NPs were 3.5, 3.4, and 3.0 nm, respectively, statistically similar to each other and C6S Pd NPs. The average core diameters of 12x, 6x, and 3x $C16NH_2$ Pd NPs were 3.0, 3.1, and 5.1 nm, respectively, showing that a low alkylamine/Pd mole ratio used during the synthesis increased the size of the $C16NH_2$ Pd NPs.[42] The size of Pd NPs coated with $C16NH_2$ did not differ statistically when the ratio was between 12:1 and 6:1 alkylamine/Pd. It is important to note that the average diameters reported in Table 1 are based on the counting of clearly isolated, individual NPs in the TEM images. Some of the NPs appeared larger, but it was not clear if that was the actual size of the NPs or if those were aggregates. In those examples, highlighted by an asterisk, we counted only clearly separated and individual NPs in the analysis, and the size may not be very accurate. Images of 1/2x C6S Pd and 12x $C16NH_2$ Pd and PdAg NPs contained mostly well-isolated NPs, but $C8NH_2$, $C12NH_2$, and 3x and 6x $C16NH_2$ Pd or PdAg NPs appeared slightly aggregated and irregular-shaped. This shows that shorter chain alkylamines and a lower ratio of the $C16NH_2$ ligands used during the synthesis leads to NPs with lower stability against aggregation.

We also synthesized PdAg NPs coated with $CnNH_2$, in which the mole ratio was 10:1 (Pd/Ag). The mole ratio of $C8NH_2$, $C12NH_2$, and $C16NH_2$ was 12:1 with respect to the total metal content (12x). EDX of PdAg NPs confirmed that the final relative composition of Pd and Ag closely matched the relative metal salt concentrations of K_2PdCl_4 and $AgC_2F_3O_2$ used in the synthesis (see Figure S-2, Supporting Information). 12x $C8NH_2$, 12x $C12NH_2$, and 12x $C16NH_2$ $Pd_{91}Ag_9$ NPs ranged in diameter from 2.5 to 2.9 nm.

The organic weight percent from TGA measurements for Pd and PdAg NPs stabilized with various organic ligands are also shown in Table 1 (column 3). For 1/2x C6S Pd, 12x $C8NH_2$ Pd, 12x $C12NH_2$ Pd NPs, and $Pd_{91}Ag_9$ alloy NPs coated with 12x $C8NH_2$ and 12x $C12NH_2$, the total organic content ranged from 17.8 to 22.0%. These values are consistent with monolayer coatings of the ligand. The organic content for 6x $C16NH_2$ Pd (57.9%), 12x $C16NH_2$ Pd (83.6%), and 12x $C16NH_2$ $Pd_{91}Ag_9$ NPs (86.9%) is too large for a single monolayer and is attributed to the formation of a full or partial bilayer of ligands on the Pd cores, as reported previously by Shuang and co-workers for octadecylamine-coated Pd NPs.[42] The higher organic content for the larger alkylamine/Pd ratio for the $C16NH_2$ ligands is consistent with less aggregation in the TEM images for these NPs. To confirm that the increased stability of $C16NH_2$ Pd and PdAg NPs was due to the formation of a bilayer of ligands rather than the presence of excess ligands not fully rinsed, we also purified the NPs by (1) rinsing copiously with 500 mL of ethanol, (2) soaking in ethanol solution overnight and further rinsing, and (3) sonicating in ethanol and further rinsing prior to filtration and collection. The TGA showed organic weight percents of 81.6, 81.4, and 68.4% for these treatments, respectively, showing that it is very difficult to remove the $C16NH_2$ ligands. Since the free ligand is highly soluble in ethanol, we believe all of the $C16NH_2$ ligands are associated with the Pd NPs and not just in excess. For some unknown reason, the ligand structure around the Pd is very different for the 6x and 3x preps based on the very different organic weight percent. Further work is needed to better understand this.

The average core diameter from the TEM images and the organic weight percent from TGA measurements allowed us to roughly estimate the composition for the NPs listed in Table 1 (column 4). Our calculations were based on a spherical model of the Pd and PdAg core, although the metal cores likely have a truncated octahedral shape containing surface defect atoms (edges and vertices).[39,40,81,82]

As described in the Experimental Section and in our previous report,[78] we synthesized mixed ligand $C8NH_2$/C6S Pd NPs with varying ratios by a liquid-phase ligand place-exchange reaction between $C8NH_2$ Pd NPs and free C6SH ligands in solution. We propose that the exchange reaction proceeds as follows, although there is no direct evidence of the detailed mechanism, which is currently not fully understood.[81,82]

$$Pd_{1455}(C8NH_2)_{280} + x\text{C6SH} \rightarrow Pd_{1455}(C8NH_2)_{280-x}(C6S)_x + x\text{C8NH}_2 + \frac{1}{2}x\text{H}_2 \quad (1)$$

Table 1 displays the estimated composition of $Pd_{1455}(C8NH_2)_{280-x}(C6S)_x$ where x was varied to be 14, 46, 95, 150, 217, 267, and 311. The number of Pd atoms, 1455, is based on the TEM measured Pd diameter of $C8NH_2$ Pd NPs. The mixed ligand composition is based on the original moles of $C8NH_2$ in the sample, the number of moles of C6SH added, and the fact that the C6SH fully replaces the $C8NH_2$ ligands. Nuclear magnetic resonance (NMR) spectroscopy confirmed this, and it is known that the Pd−S−R bond is much stronger compared with Pd−NH_2−R.[78]

Hydrogen Stability of $CnNH_2$ Pd NPs. UV−vis spectroscopy and TEM imaging provided information about the stability of Pd NPs in solution in the presence of H_2 for different amounts of time. We studied the stability only in H_2, since it is one of the reactants for the hydrogenation/isomerization of allyl alcohol and it is known that large morphology changes and aggregation can occur with Pd in the presence of H_2 due to the formation of PdH_x.[77,78] Figure 1 shows normalized UV−vis spectra of toluene solutions containing 12x $C8NH_2$ Pd and 12x $C16NH_2$ Pd NPs, which were exposed to 100% H_2 at a constant flow of 8.0 ± 0.2 mL/min for 0, 5, 15, 30, and 60 min. The spectrum of the 12x $C8NH_2$ Pd NPs exhibited a dramatic absorbance decrease during H_2 exposure for 60 min (frame A) due to H_2-induced aggregation and precipitation, as we previously reported.[78] In contrast, the spectrum of the 12x $C16NH_2$ Pd NPs (frame B) changed minimally, indicating higher stability for the latter due to the longer chain length and high organic content based on TGA (full or partial bilayer).

Figure 2 shows plots of the normalized absorbance at 310 nm of toluene solutions of C6S Pd and $CnNH_2$ Pd NPs of varied chain length (frame A) and varied alkylamine/Pd ratios for $C16NH_2$ Pd NPs (frame B) as a function of exposure time to pure H_2 bubbling through the solution at a flow rate of 8.0 ± 0.2 mL/min. The points and curves represent the average of three samples prepared with the standard deviations shown. The absorbance of 12x $C8NH_2$ Pd NPs decreased rapidly with time, almost reaching zero after 60 min, as also shown in Figure 1A.[78] As the carbon chain length of the alkylamine ligands on the NPs increased, the overall stability against aggregation increased. The 12x $C12NH_2$ Pd NPs displayed a stable

dx.doi.org/10.1021/cs300361y | ACS Catal. 2012, 2, 2602−2613

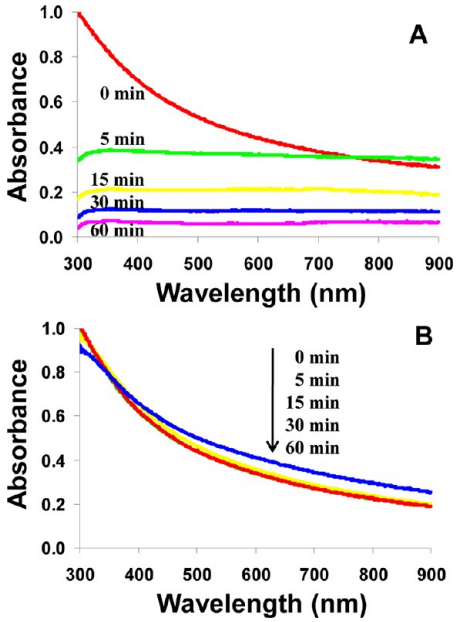

Figure 1. UV−vis spectra of a toluene solution of (A) $C8NH_2$ Pd NPs and (B) $C16NH_2$ Pd NPs synthesized with a 12:1 $CnNH_2$/Pd ratio (12x) before and after exposure to 100% H_2 at a flow rate of 8.0 ± 0.2 mL/min for different times.

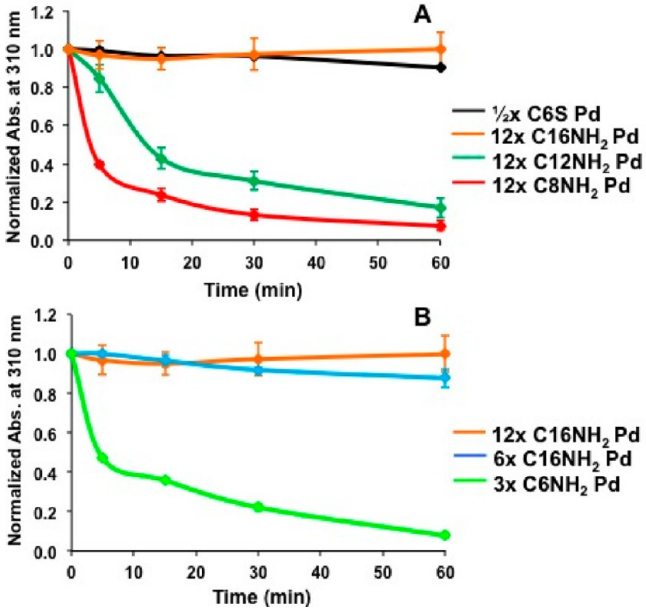

Figure 2. Plots of the normalized absorbance at 310 nm of toluene solutions containing (A) C6S Pd NPs and $CnNH_2$ Pd NPs synthesized with a 1:2 C6S/Pd ratio (1/2x) and a 12:1 $CnNH_2$/Pd ratio (12x) and (B) $C16NH_2$ Pd NPs prepared at various ligand/metal ratios (12:1, 12x; 6:1, 6x; 3:1, 3x) versus exposure time to 100% H_2 at a flow rate of 8.0 ± 0.2 mL/min.

absorbance at $A \sim 0.2-0.4$, showing that most of the Pd NPs became insoluble. The normalized absorbance of the solutions of 12x $C16NH_2$ Pd and 1/2x C6S Pd NPs was stable at $A \sim 0.8-0.9$ after 60 min, indicating high stability against aggregation in the presence of H_2. The high stability of C6S Pd NPs against H_2-induced aggregation is due to the strongly coordinated thiolates, preventing reactivity of Pd with H_2 or inhibiting aggregation of PdH_x NPs.[57] In the case of Pd NPs coated with $C16NH_2$, the high stability of the NPs is attributed to the long carbon chain length of the alkylamine ligand and the formation of a bilayer, which can reduce the chance of collisions and aggregation of the Pd NPs. In frame B, the normalized absorbance of 3x $C16NH_2$ Pd NPs decreased dramatically with time, suggesting that the Pd NPs were not well protected by the $C16NH_2$ in this case. This was accompanied by the noticeable precipitation of the NPs (see Figure S-3, Supporting Information). This is consistent with the low organic content determined by TGA (14.4%). As the number of $C16NH_2$ ligands on the Pd NPs increased, as determined by TGA, the rate of aggregation decreased. Accordingly, the 6x and 12x $C16NH_2$ Pd NPs were significantly more stable in the presence of H_2. It is not clear why the 3x $C16NH_2$ Pd NPs had such a low organic content.

To further determine if the $C16NH_2$ ligands are associated with the Pd NPs in the 6x and 12x preps or if they are just excess ligands, we monitored the stability of $C8NH_2$ Pd NPs with excess $C8NH_2$ ligands intentionally added to the solution to increase the total organic content to 66.4% and 82.0%. The $C8NH_2$ Pd NPs still precipitated by 60 min, but the rate of precipitation was decreased as the organic content increased, as shown in Figure S-4 of the Supporting Information. The fact that they were still not fully stable shows that the total organic content is not the only factor needed to stabilize the Pd NPs. There is something different about the $C16NH_2$ ligands, which we believe is the ability to form a fairly stable bilayer associated with the Pd NP surface. This experiment provides indirect evidence of that.

We used TEM to directly correlate the UV−vis data with the morphology of the Pd NPs. Figure 3 displays TEM images of

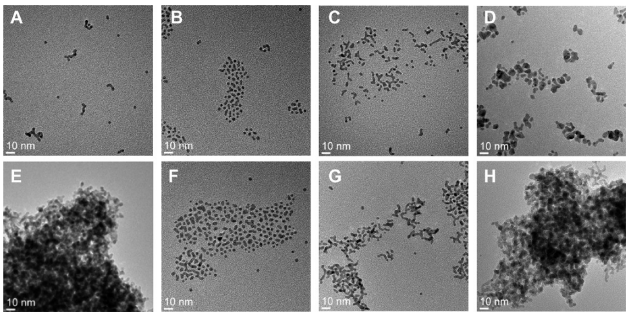

Figure 3. TEM images of drop-cast films of 12x $C12NH_2$ Pd, 12x $C16NH_2$ Pd, 6x $C16NH_2$ Pd, and 3x $C16NH_2$ Pd NPs before (A, B, C, D) and after exposure to 100% H_2 for 60 min (E, F, G, H).

Pd NPs prepared with different types of $CnNH_2$ ligands before (A−D) and after H_2 exposure (E−H). Figure 3A and B shows TEM images of 12x $C12NH_2$ and 12x $C16NH_2$ Pd NPs, respectively, before H_2 exposure. Both samples show the presence of metal NPs in the 3.0 to 3.4 nm diameter size range. Several of the 12x $C12NH_2$ Pd NPs appear slightly aggregated (frame A), as also observed previously for 12x $C8NH_2$ Pd NPs.[78] In contrast, all of the 12x $C16NH_2$ Pd NPs are well isolated and spherical (frame B). Figure 3E and F shows the images of the corresponding samples after exposure to 100% H_2 for 60 min at a constant flow of 8.0 ± 0.2 mL/min. The image of the 12x $C12NH_2$ Pd NPs (frame E) shows that the NPs aggregated into large superstructures, and there was no evidence of individual, isolated NPs in the images. The image of the 12x $C16NH_2$ Pd NPs (frame F) shows several well-isolated NPs and a few that have undergone some slight

dx.doi.org/10.1021/cs300361y | ACS Catal. 2012, 2, 2602−2613

enlargement. Figure 3C and D shows TEM images of 6x and 3x $C16NH_2$ Pd NPs, respectively, before H_2 exposure whereas Figure 3G and H shows images of the corresponding samples after exposure to H_2 for 60 min. As the $C16NH_2$/Pd ratio (6:1 and 3:1) decreased during the synthesis, the rate of aggregation increased, and the Pd NPs exhibited significant morphology changes before and after H_2 exposure. In particular, the NPs synthesized with a 3:1 $C16NH_2$/Pd ratio were the largest and most heavily aggregated after H_2 exposure, forming structures with dimensions in the several hundred nanometer to micrometer size range, similar to those observed for 12x $C8NH_2$ and 12x $C12NH_2$ Pd NPs. In fact, these NPs even appeared aggregated after drying on the TEM grid without exposure to H_2 (Figure 3D), indicating lower stability. The images in Figure 3 are consistent with the UV−vis data.

Hydrogen Stability of $CnNH_2$ PdAg NPs. We next studied the H_2 stability of PdAg NPs in solution. These alloys are significant because Ag has the ability to adsorb large amounts of H_2 into its lattice if Pd atoms are present to catalyze the breaking of the H−H bond.[83,84] Another added benefit of this alloy is that Ag is much cheaper than Pd, which could reduce the cost of catalysts based on these materials. Figure 4 shows the change in absorbance of toluene solutions of 12x $C16NH_2$, 12x $C12NH_2$, and 12x $C8NH_2$ PdAg NPs as a function of exposure time to 100% H_2 bubbling through the solution at 8.0 mL/min. The $C16NH_2$ $Pd_{91}Ag_9$ NPs displayed a minimal change in absorbance and high stability against aggregation in the presence of H_2, as shown for pure $C16NH_2$ Pd NPs (Figure 2). In the case of $Pd_{91}Ag_9$ NPs coated with $C12NH_2$ and $C8NH_2$, the absorbance decreased slowly with time, almost reaching $A \sim 0.2-0.3$ after 60 min of H_2 exposure. Interestingly, this decrease was more gradual than that observed for pure Pd alkylamine MPC solutions in Figure 2A, showing some enhanced stability by adding a small amount of Ag. This is consistent with previous conductivity and IR data of these NPs in the presence of H_2.[77]

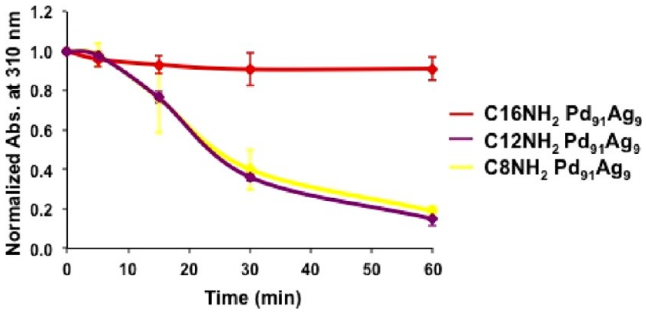

Figure 4. Plots of the normalized absorbance at 310 nm of toluene solutions containing $CnNH_2$ PdAg NPs versus exposure time to 100% H_2 at a flow rate of 8.0 ± 0.2 mL/min. The $CnNH_2$/PdAg mole ratio was 12:1 (12x). The mole ratio between Pd and Ag was 10:1.

Figure 5 shows TEM images of PdAg NPs synthesized with 12x $C16NH_2$, 12x $C12NH_2$, and 12x $C8NH_2$ before (A−C) and after H_2 exposure (D−F). Frames A, B, and C show TEM images of $Pd_{91}Ag_9$ NPs coated with $C16NH_2$, $C12NH_2$, and $C8NH_2$ ligands, respectively, before H_2 exposure. These NPs were well-isolated and spherical; however, several of the $C12NH_2$ and $C8NH_2$ $Pd_{91}Ag_9$ NPs appeared slightly aggregated (frames B and C), even without H_2 exposure. After exposure to 100% H_2 for 60 min, only the $C16NH_2$ $Pd_{91}Ag_9$ NPs remained well isolated and spherical, with some minor evidence of aggregation, whereas the other two samples were heavily aggregated, consistent with the UV−vis data in Figure 4.

Hydrogen Stability of $C8NH_2$/C6S Mixed Ligand Pd NPs. In our previous report, we studied the reactivity and stability of $C8NH_2$/C6S Pd NPs to H_2 gas by UV−vis spectroscopy, TEM, and electronic conductivity measurements.[78] Figure S-5 of the Supporting Information shows normalized UV−vis spectra of diluted toluene solutions containing $C8NH_2$/C6S Pd NPs of varied ratios (266/14, 234/46, 185/95, 130/150, 63/217, 13/267, and 0/311) that were exposed to 100% H_2 at a flow rate of 8.0 ± 0.2 mL/min for 60 min. The change in absorbance of the solutions depended on the $C8NH_2$/C6S ratios. For $C8NH_2$/C6S ratios of 266/14 and 234/46, the Pd NPs precipitated significantly, displaying a stable absorbance at $A \sim 0.1-0.3$ after 60 min. Pd

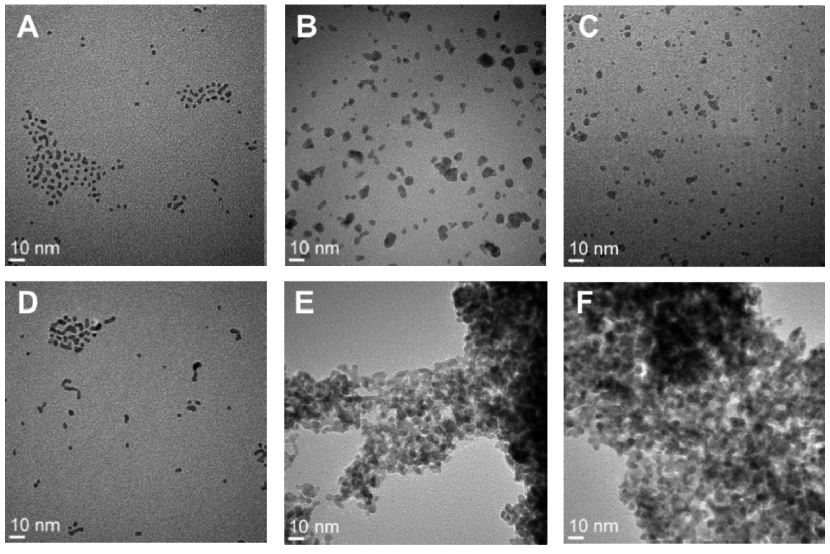

Figure 5. TEM images of drop-cast films of 12x $C16NH_2$, 12x $C12NH_2$, and 12x $C8NH_2$ $Pd_{91}Ag_9$ NPs before (A, B, C) and after exposure to 100% H_2 for 60 min (D, E, F).

dx.doi.org/10.1021/cs300361y | ACS Catal. 2012, 2, 2602−2613

NPs coated with ligand ratios of 130/150, 63/217, 13/267, and 0/311 remained much more stable for the entire 60 min time period ($A \sim 0.8-1.0$). For the 185/95 $C8NH_2$/C6S Pd NPs, the absorbance decreased by ~50% after 60 min of H_2 bubbling. These interesting data indicate that partial coverage with C6S ligands (at least 150 out of 280) provides fairly good stability against H_2-induced aggregation, as reported previously.[78]

Catalysis Experiments. To investigate the catalytic properties, we studied the reaction of 2-propen-1-ol with H_2 in the presence of the various Pd and PdAg NPs as catalysts. Because this allyl alcohol is the simplest α,β-unsaturated alcohol and has been used as a substrate in prior studies,[30,31,33,34,40,44,45,58−62,64−66] it was a good starting point for this work. As illustrated in Scheme 3, the reaction between allyl alcohol and H_2 (g) using Pd catalysts results in the hydrogenation of the double bond to give propanol, but it may also lead to migration of the double bond (isomerization), yielding the corresponding saturated aldehyde.[70,71] Although heterogeneous Pd catalysts, such as Pd/TiO_2,[75,85] polymer−Pd(0) and Pd(II) complexes,[76] and Pd NPs stabilized by polymers and immobilized on composites[33,66,67] or embedded in polyelectrolyte films,[60,80,86,87] have been used to study the activity and selectivity for hydrogenation and isomerization of allyl alcohols, the favored hydrogenation process prohibited formation of the isomer. An important challenge is to controllably obtain the alcohol or the saturated carbonyl derivatives, which are essential compounds in organic synthesis.[69−73] Therefore, our goal was to better understand the catalytic process with different Pd and Pd alloy NPs and to control the selectivity and improve the reaction rate by designing different, stable NPs.

Scheme 3. Conversion of Allyl Alcohol to the Saturated Alcohol and Aldehyde by Catalytic Reactions

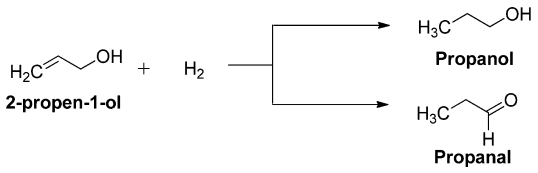

As reported previously, the formation of a surface palladium hydride species (PdH_x), either isolated or generated in situ, is a fundamental requirement in the hydrogenation and isomerization of allyl alcohols.[75,85] This was confirmed by the fact that we observed no reaction over our Pd and PdAg NPs in the absence of H_2. We also observed no reaction with H_2 without the NP catalyst present. Pure H_2 was bubbled through a CH_2Cl_2 solution containing allyl alcohol and catalyst at a flow rate of 8.0 ± 0.2 mL/min, and the reactions were monitored by gas chromatography (GC). As an example, Figure 6 shows chromatograms obtained before and after 15, 30, 60, and 100 min of reaction with 1/2x C6S Pd and 12x $C8NH_2$ Pd NPs as catalysts in frames A and B, respectively. With C6S Pd, the peak for allyl alcohol at 3.70 min decreased with time while a peak at 1.13 min corresponding to the aldehyde increased. C6S Pd NPs are clearly active catalysts and selective for the isomerization reaction (Scheme 3, propanal). The small change in the UV−vis, TEM, and previous conductivity studies suggested some reactivity with H_2, but the GC data confirms that these NPs are active catalysts.[77,78] Shon and co-workers recently described the same selectivity with alkanethiolate-capped Pd NPs prepared from Bunte salts.[58,59] With 12x $C8NH_2$ Pd NPs, the peak for allyl alcohol also decreased (frame B), but two peaks appeared at 1.26 and 3.12 min, corresponding to the aldehyde and alcohol, respectively, in about a 50:50 ratio (see Figure S-6, Supporting Information). This shows that both isomerization and hydrogenation reactions took place with $C8NH_2$ Pd NP catalysts. Importantly, these NPs are active catalysts, and the nature of the ligand strongly affects the reaction product.

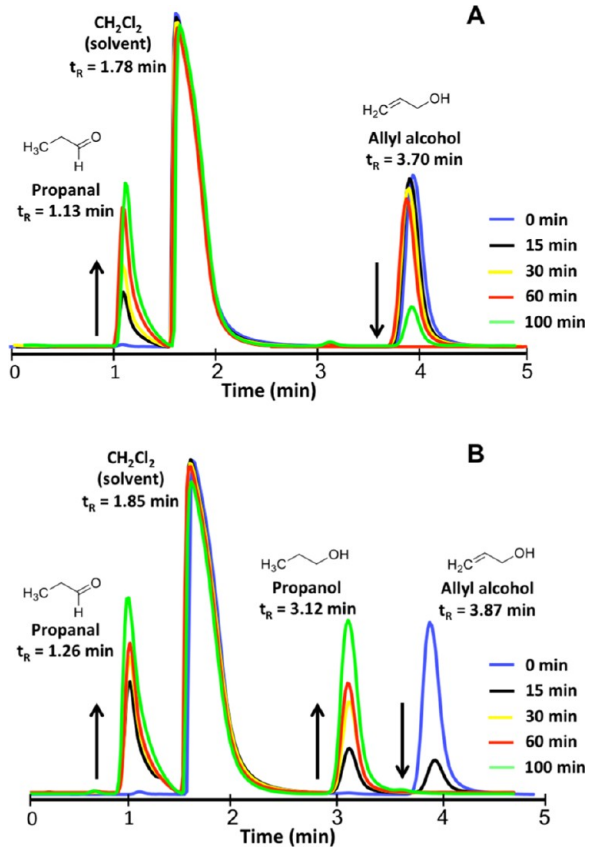

Figure 6. Gas chromatograms showing progress of catalytic reaction of allyl alcohol before and after exposure to 100% H_2 at different reaction times. The reaction was catalyzed by ~3.0 mg of (A) 1/2x C6S Pd NPs and (B) 12x $C8NH_2$ Pd NPs in 4 mL of CH_2Cl_2 under atmospheric pressure and at room temperature. Integration was performed using instrument software. Injection volume = 1 μL, initial temperature = 60 °C, final temperature = 135 °C, ramp = 15 °C/min, pressure = 20 PSI, detector = FID.

Selectivity of C6S and $CnNH_2$ Pd and PdAg NPs. We conducted the experiment shown in Figure 6 on all of the Pd NP catalysts synthesized. Figure 7 displays the selectivity toward hydrogenation and isomerization products after 100 min of reaction. The reaction went to 100% completion within this time using all of the catalysts, except for the C6S Pd NPs (91% completion) and the 3x $C16NH_2$ Pd NPs (98% completion). The results generally indicate that the selectivity depends on both ligand composition and metal composition.

Figure 7A shows a comparison between the selectivity of 1/2x C6S Pd, 12x $C8NH_2$ Pd, 12x $C12NH_2$ Pd, and 12x, 6x, and 3x $C16NH_2$ Pd NPs. The Pd NPs coated with C6S ligands selectively catalyzed the formation of the aldehyde (98%). In contrast, the reaction using $CnNH_2$ Pd NPs gave both hydrogenation and isomerization products in about 5:5 or 6:4 ratios. This was true even after a prolonged reaction time of 5 h,

dx.doi.org/10.1021/cs300361y | ACS Catal. 2012, 2, 2602−2613

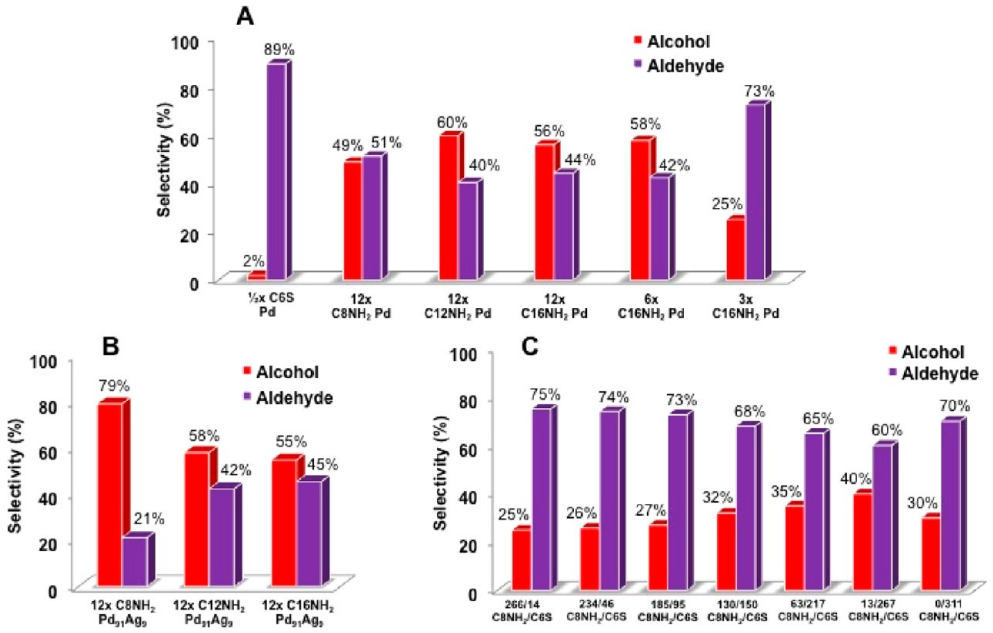

Figure 7. Selectivity toward hydrogenation and isomerization products after 100 min of reaction between allyl alcohol and 100% H_2 (8.0 ± 0.2 mL/min) over (A) C6S Pd and $CnNH_2$ Pd NP catalysts with different alkylamine/Pd ratios (12x, 6x, 3x), (B) PdAg NPs coated with $CnNH_2$ (12:1 alkylamine/PdAg ratio, 12x), and (C) Pd NP catalysts coated with various $C8NH_2$/C6S ratios.

showing that the aldehyde is not an intermediate to the alcohol product. Interestingly, the 3x $C16NH_2$ Pd NPs were slightly more selective to the aldehyde (73%) for reasons not understood.

We also compared the selectivity of 12x $CnNH_2$ PdAg NPs as shown in Figure 7B. 12x $C8NH_2$ $Pd_{91}Ag_9$ NPs selectively catalyzed the alcohol (79%) over the aldehyde (21%). Interestingly, the addition of Ag to the Pd NP catalyst increased the selectivity toward the hydrogenation reaction. However, $Pd_{91}Ag_9$ NPs coated with 12x $C12NH_2$ and 12x $C16NH_2$ ligands showed both hydrogenation and isomerization products in about a 6:4 ratio, showing that the ligand chain length also plays an important role.

Selectivity of $C8NH_2$/C6S Mixed Ligand Pd NPs. Figure 7C shows the selectivity of the mixed ligand Pd NPs with $C8NH_2$/C6S ratios of approximately 266/14, 234/46, 185/95, 130/150, 63/217, 13/267, and 0/311. The reaction went to 100% completion within 100 min, and the selectivity favored the aldehyde (60−75%) over the alcohol (25−40%) in all cases. It is interesting that the incorporation of only 14 C6S ligands into the $C8NH_2$ Pd NPs altered the selectivity from 51% aldehyde for pure $C8NH_2$ to 75% aldehyde for a $C8NH_2$/C6S ratio of 266/14. This shows that a small amount of ligand additives could be a promising route to alter the selectivity and stability of metal NP catalysts.

Catalytic Activity of C6S and $CnNH_2$ Pd and PdAg NPs. The turnover frequencies (TOFs, mol substrate/mol Pd/hour) of the conversion of allyl alcohol to the corresponding hydrogenation and isomerization products (propanol and propanal, respectively) in the presence of H_2 and C6S Pd and $CnNH_2$ Pd and PdAg NPs are displayed in Table 2. The TOFs varied significantly, depending on the ligand and metal composition of the NPs. It is useful to first note the difference between NPs that were stable (soluble) during the reaction (indicated by an asterisk) and those that were unstable (became insoluble) during the reaction (indicated by "NS"). Those that were unstable in H_2 only were also not stable during the catalysis reaction, which includes $C8NH_2$, $C12NH_2$, and 3x $C16NH_2$ Pd and PdAg NPs. It is interesting that 6x $C16NH_2$ Pd NPs were stable in H_2 only, but not stable during the catalysis reaction, showing that the reaction of allyl alcohol at the Pd NP surface can also contribute to NP instability. The clear trend in the $CnNH_2$ Pd and PdAg NPs is that the total TOF increased with increasing NP stability. The $C12NH_2$ Pd displayed a greater TOF compared with the $C8NH_2$ Pd because of greater stability imparted by the longer chain length. When comparing the same $C8NH_2$ or $C12NH_2$, the PdAg NPs displayed higher TOF values compared with the Pd NPs. This is also due to the greater stability of the PdAg NPs, as shown by the UV−vis data. The largest total TOF in this series was 384 from the most stable 6x $C16NH_2$ Pd NPs. Those eventually precipitated but took the longest to do so. Low stability leads to

Table 2. Hydrogenation and Isomerization Rates of Allyl Alcohol by C6S Pd and $CnNH_2$ Pd and PdAg NPs

	TOF (mol substrate/mol Pd/h)[a]		
nanoparticles[b]	hydrogenation	isomerization	total[c]
1/2x C6S Pd*	0	46.7 ± 12.0	46.7
12x $C8NH_2$ Pd^{NS}	38.3 ± 4.1	81.4 ± 11.6	119.7
12x $C12NH_2$ Pd^{NS}	61.2 ± 17.0	132.8 ± 5.1	194.0
3x $C16NH_2$ Pd^{NS}	27.8 ± 10.5	85.7 ± 20.0	113.5
6x $C16NH_2$ Pd^{NS}	99.0 ± 10.5	284.6 ± 0.9	383.6
12x $C16NH_2$ Pd*	158.4 ± 11.1	560.1 ± 85.9	718.5
12x $C8NH_2$ $Pd_{91}Ag_9^{NS}$	63.2 ± 3.1	89.5 ± 1.8	152.7
12x $C12NH_2$ $Pd_{91}Ag_9^{NS}$	61.1 ± 0.2	163.7 ± 4.2	224.8
12x $C16NH_2$ $Pd_{91}Ag_9$*	371.6 ± 9.3	605.3 ± 178.3	976.9

[a]The TOFs (mol substrate/mol Pd/h) are initial values determined at total conversion of less than 60% (see Figure S-7, Supporting Information). The TOFs represent the average of three samples analyzed for each catalyst. [b]NS (not stable) = these NPs precipitated during the course of the reaction. * = these NPs were stable during the course of the reaction. [c]Total values represent the sum of TOF for hydrogenation and isomerization.

dx.doi.org/10.1021/cs300361y | ACS Catal. 2012, 2, 2602−2613

low total TOF values because aggregated NPs have less surface area available and are less reactive. The stability provided by the longer-chain-length alkylamines is more beneficial compared with the possible negative effects of the larger barrier properties of the longer-chain-length alkylamines since the $C12NH_2$ Pd and PdAg NPs have larger TOF values as compared with the $C8NH_2$ Pd and PdAg NPs.

The C6S Pd and 12x $C16NH_2$ Pd and PdAg NPs were stable in H_2 only and during the catalysis reaction (see Figures S-8 and S-9, Supporting Information). In the case of the 12x $C16NH_2$ Pd NPs, the same trend holds that the 12x $C16NH_2$ Pd had a larger total TOF compared with the shorter 12x $C12NH_2$ and $C8NH_2$ Pd NPs because of the greater stability afforded by the longer chain. That is more important than the fact that the longer chain might inhibit access of allyl alcohol to the Pd surface, which is apparently not a problem. The $C16NH_2$ PdAg NPs were again more stable than the pure Pd NPs because of the greater stability of the PdAg. These displayed the highest total TOF of all the Pd NPs at 977 mol substrate/mol Pd/h. While highly stable, the C6S Pd NPs displayed the lowest total TOF value because of the strong coordination of the thiolate to the Pd surface. Comparing this to the $C16NH_2$ Pd NPs shows that strong coordination to the metal surface is more detrimental to its catalytic activity when compared with a long chain length. With a long chain length but weak coordinating ligand, such as the amine, the allyl alcohol readily reacts with the Pd NPs, but with a short chain length but strong coordinating thiol, the reactivity is greatly diminished by a factor of 20 down to a TOF value of 47 mol substrate/mol Pd/h. NP size may also be an important factor,[20,21,34,45,60] but was not controlled in this study.

Catalytic Activity of Mixed Ligand $C8NH_2$/C6S Pd NPs. Table 3 shows the TOF values for the hydrogenation, isomerization, and total TOF using the different mixed $C8NH_2$/C6S Pd NPs as catalysts. It is important to note that although Pd NPs with $C8NH_2$/C6S ratios of 130/150, 63/217, 13/267, and 0/311 were all stable in the presence of H_2 only, only the 0/311 ratio was stable during the catalysis reaction. This again shows that the reaction of allyl alcohol at the Pd NP surface can lead to NP instability. Figure S-9 of the Supporting Information shows UV−vis spectra of the various mixed monolayer Pd NPs in H_2 only as compared with H_2 plus allyl alcohol to demonstrate this point. More work is needed to better understand all of the factors leading to NP instability.

Table 3. Hydrogenation and Isomerization Rates of Allyl Alcohol by Mixed Ligand $C8NH_2$/C6S Pd NPs

	TOF (mol substrate/mol Pd/h)[a]		
nanoparticles[b]	hydrogenation	isomerization	total[c]
Pd $(C8NH_2)_{266}$ $(C6S)_{14}^{NS}$	24.7 ± 5.5	79.5 ± 14.0	104.2
Pd $(C8NH_2)_{234}$ $(C6S)_{46}^{NS}$	36.5 ± 1.9	100.0 ± 5.4	136.5
Pd $(C8NH_2)_{185}$ $(C6S)_{95}^{NS}$	33.7 ± 0.3	92.1 ± 9.6	125.8
Pd $(C8NH_2)_{130}$ $(C6S)_{150}^{NS}$	38.2 ± 8.1	106.5 ± 8.9	144.7
Pd $(C8NH_2)_{63}$ $(C6S)_{217}^{NS}$	24.0 ± 3.5	83.1 ± 2.4	107.1
Pd $(C8NH_2)_{13}$ $(C6S)_{267}^{NS}$	15.5 ± 2.7	30.2 ± 5.9	45.7
Pd $(C8NH_2)_0$ $(C6S)_{311}$*	10.8 ± 1.6	21.7 ± 1.1	32.5

[a]The TOFs (mol substrate/mol Pd/h) are initial values determined at total conversion of less than 60%. The TOFs represent the average of three samples analyzed for each catalyst. [b]NS (not stable) = these NPs precipitated during the course of the reaction. * = these NPs were stable during the course of the reaction. [c]Total values represent the sum of TOF for hydrogenation and isomerization.

When comparing the different $C8NH_2$/C6S Pd NPs, there is a trade-off between stability provided by the C6S ligands and inhibition of the reactivity from the strongly coordinated thiolate group. In terms of the total TOF value, the highest value of 145 mol substrate/mol Pd/h occurred for the $C8NH_2$/C6S ratio of 130/150. This may be optimal since there are enough C6S ligands to improve the stability of the Pd NPs relative to $C8NH_2$ only, and there are also enough $C8NH_2$ ligands on the Pd NP surface to allow reactivity with allyl alcohol. Although this is the optimal ratio in terms of total TOF, the TOF is still much lower compared with $C16NH_2$ Pd and PdAg NPs, and they precipitate during the reaction. Unfortunately, the mixed monolayer strategy did not lead to Pd NPs with both high reactivity and high stability, as hoped. It seems that the thiol groups still inhibit the reactivity, and the amines still lead to instability, with only a minor improvement. The $C8NH_2$/C6S ratio of 0/311 should lead to Pd NPs completely coated with C6S ligands with some excess C6S also in solution. While these are highly stable, they are not highly reactive (similar to the as-synthesized C6S Pd NPs) because of the strongly coordinated thiols. They are actually worse than the C6S Pd NPs because of the excess thiols in solution.

Comparison with Other Nanoparticle Catalysts. Bruening and co-workers reported the TOFs for the hydrogenation of allyl alcohol with Wilkinson's catalyst, which is a common homogeneous catalyst.[80] They determined that Wilkinson's catalyst had a minor selectivity toward the formation of the isomer of allyl alcohol. Although the rates of hydrogenation of allyl alcohol obtained with our synthesized Pd and PdAg NPs compare very well with Wilkinson's catalysts, the selectivity and activity toward the formation of the hydrogenation and isomerization products could be controlled by changing the ligand composition and metal composition of the NPs. For instance, we observed that Pd NPs coated with C6S ligands favored the formation of the isomer, giving 98% propanal after 100 min of reaction (Figure 7), but had low TOF (47 mol substrate/mol Pd/h). Shon and co-workers reported the same selectivity for dodecanethiolate-capped Pd NPs generated from thiosulfate in the isomerization of allyl alcohol, for which the reaction was 80% complete after 1 h.[58,59]

Zharmagambetova and co-workers reported 74% propanal when Pd−polymer complexes containing iminodithiol were used as catalysts.[76] In the case of the homogeneous 12x $C16NH_2$ Pd and PdAg NP catalysts, the selectivity to the alcohol was 60%, which is lower than that of the commercial hydrogenation catalysts with high surface area, such as Pd/C[62,65] and Pd/Al_2O_3 (~75%).[62,76] However, these NP catalysts exhibited higher activity (TOF = 700−1000), with $C16NH_2$ $Pd_{91}Ag_9$ NPs being the best, compared with the activity of other homogeneous systems previously investigated including Pd and Pt NPs stabilized by dendrimers[31,44] and alkanethiolate monolayers[40,58,59] (TOF < 500). Other studies have reported TOF ≫ 1000 when hollow polystyrene nanospheres[61] and collagen fiber[62] coated with Pd NPs were used to catalyze the hydrogenation of allyl alcohol. The reactions were carried out under different conditions, but these are clearly promising strategies for Pd catalysis.

Our motivation for making Pd-containing alloy NPs was based not only on increasing the atom economy of the catalyst, but also on the possibility of enhancing its selectivity and activity. Other groups have investigated the catalytic activity of

dx.doi.org/10.1021/cs300361y | ACS Catal. 2012, 2, 2602−2613

bimetallic NPs (PdAu,[58] PdPt,[88,89] and AgPd[90]) for the selective hydrogenation of allyl alcohols. For example, Crooks and co-workers demonstrated that Pd−Pt dendrimer-encapsulated NPs have higher catalytic activity than dendrimer-encapsulated Pd or Pt NPs for the hydrogenation of allyl alcohol.[88] We observed that when 12x $C8NH_2$ $Pd_{91}Ag_9$ NPs were used, the complete consumption of allyl alcohol required 100 min, and 80% alcohol was obtained with a hydrogenation rate 2 times faster compared with the corresponding pure Pd NPs. Scott and co-workers determined that the presence of Ag on AgPd NP catalysts prepared by galvanic exchange dramatically improved the selectivity for hydrogenation over the isomerization product, and the overall rate of hydrogenation was enhanced, which is in agreement with our results.[90]

CONCLUSIONS

We studied the stability of solutions of chemically synthesized C6S Pd and $CnNH_2$ (n = 8, 12, and 16) Pd and PdAg NPs in the presence of H_2 by UV−vis spectroscopy and TEM measurements. Although C6S Pd NPs show high stability against H_2-induced aggregation, the rate of aggregation for Pd and PdAg NPs coated with $CnNH_2$ depends on the ligand and metal composition of the NPs. Among the $CnNH_2$ Pd and PdAg NPs, the 6x and 12x $C16NH_2$ Pd and $Pd_{91}Ag_9$ NPs exhibit the highest stability in the presence of H_2. This is attributed to the long carbon chain length and the high coverage of the alkylamine ligands on the NPs, which form a full or partial bilayer that prevents the NP aggregation. The Pd and PdAg NPs could directly be used to catalyze the hydrogenation and isomerization of allyl alcohol with H_2 in solution to give propanol and propanal, respectively. C6S Pd NP catalysts show high selectivity to propanal, but low activity (TOFs) because of the strong Pd−S interaction, which inhibits the reaction. All alkylamine-coated Pd NPs lead to a mixture of propanol and propanal in about 5:5, 6:4, or 3:7 ratios, depending on the ligand composition. The 12x $C16NH_2$ Pd and $Pd_{91}Ag_9$ NPs have the highest TOFs, due to high stability and weakly coordinated alkylamines. $C8NH_2$ $Pd_{91}Ag_9$ NPs favor the formation of the saturated alcohol, but have low stability. The mixed ligand $C8NH_2$/C6S Pd NPs were stable in the presence of H_2 only for 150 C6S ligands or more, but not highly stable during the catalysis reaction. This led to selectivities similar to C6S Pd NPs, which favor the aldehyde, and TOF values similar to, but slightly larger than, $C8NH_2$ Pd NPs.

In summary, this study shows that the selectivity and catalytic activity of Pd and PdAg NP catalysts for hydrogenation or isomerization of allyl alchol can be controlled by simply modifying the ligand and metal composition of the NPs. In general, strong coordination of the capping ligands and low NP stability inhibit reactivity far greater than a long alkyl chain surrounding the Pd NP. The alkyl chain of the stabilizer can be quite long and the NP a highly active catalyst, provided that the NP is stable and the stabilizer is weakly coordinated to the NP. It is also clear from this work that NPs that are stable in the presence of H_2, one of the reactants, may still become unstable during the hydrogenation or isomerization reaction occurring at the NP surface. Future experiments will explore the effect of H_2 flow in the catalytic reaction, recyclability of the catalysts, other organic substrates, other alloys, and NP size to produce the most stable/active catalysts.

ASSOCIATED CONTENT

Supporting Information

TEM images of Pd and PdAg NPs, EDX analysis of PdAg NPs, digital photo of dilute toluene solutions of 12x and 3x $C16NH_2$ Pd NPs before and after H_2 bubbling for 60 min at a constant flow of 8.0 ± 0.2 mL/min, stability data for $C8NH_2$ Pd NPs with excess $C8NH_2$ in solution, UV−vis of solutions of $C8NH_2$/C6S Pd NPs in the presence of H_2, an example TOF calculation for the hydrogenation and isomerization of allyl alcohol, and stability data for various Pd and PdAg NPs in the presence of H_2 only and H_2 plus allyl alcohol. This material is available free of charge via the Internet at http://pubs.acs.org.

AUTHOR INFORMATION

Corresponding Author

*Fax: 502-852-8149. E-mail: f.zamborini@louisville.edu.

Notes

The authors declare no competing financial interest.

ACKNOWLEDGMENTS

We gratefully acknowledge the Kentucky Science and Engineering Foundation (KSEF-2012-RDE-012) for financial support of this research. We thank the Conn Center for Renewable Energy Research at the University of Louisville for use of the TGA and TEM facilities. We also thank Dr. William N. Richmond from the Department of Chemistry at the University of Louisville for his help with the gas chromatography experiments.

REFERENCES

(1) Bönnemann, H.; Richards; Ryan, M. *Eur. J. Inorg. Chem.* **2001**, 2455.
(2) Chen, H. M.; Liu, R.-S. *J. Phys. Chem. C* **2011**, *115*, 3513.
(3) Ohara, S.; Hatakeyama, Y.; Umetsu, M.; Sato, K.; Naka, T.; Adschiri, T. *J. Power Sources* **2009**, *193*, 367.
(4) Ibañez, F. J.; Zamborini, F. P. *ACS Nano* **2008**, *2*, 1543.
(5) Ibañez, F. J.; Gowrishetty, U.; Crain, M. M.; Walsh, K. M.; Zamborini, F. P. *Anal. Chem.* **2005**, *78*, 753.
(6) Walt, D. R. *ACS Nano* **2009**, *3*, 2876.
(7) Rieter, W. J.; Taylor, K. M. L.; An, H.; Lin, W.; Lin, W. *J. Am. Chem. Soc.* **2006**, *128*, 9024.
(8) Rieter, W. J.; Pott, K. M.; Taylor, K. M. L.; Lin, W. *J. Am. Chem. Soc.* **2008**, *130*, 11584.
(9) Arruebo, M.; Fernández-Pacheco, R.; Ibarra, M. R.; Santamaría, J. *Nano Today* **2007**, *2*, 22.
(10) Kievit, F. M.; Zhang, M. *Acc. Chem. Res.* **2011**, *44*, 853.
(11) Gu, F. X.; Karnik, R.; Wang, A. Z.; Alexis, F.; Levy-Nissenbaum, E.; Hong, S.; Langer, R. S.; Farokhzad, O. C. *Nano Today* **2007**, *2*, 14.
(12) Yamauchi, M.; Kobayashi, H.; Kitagawa, H. *ChemPhysChem* **2009**, *10*, 2566.
(13) Horinouchi, S.; Yamanoi, Y.; Yonezawa, T.; Mouri, T.; Nishihara, H. *Langmuir* **2006**, *22*, 1880.
(14) Zlotea, C.; Campesi, R.; Cuevas, F.; Leroy, E.; Dibandjo, P.; Volkringer, C.; Loiseau, T.; Férey, G. r.; Latroche, M. *J. Am. Chem. Soc.* **2010**, *132*, 2991.
(15) Kesavan, L.; Tiruvalam, R.; Rahim, M. H. A.; bin Saiman, M. I.; Enache, D. I.; Jenkins, R. L.; Dimitratos, N.; Lopez-Sanchez, J. A.; Taylor, S. H.; Knight, D. W.; Kiely, C. J.; Hutchings, G. J. *Science* **2011**, *331*, 195.
(16) Pasquato, L.; Pengo, P.; Scrimin, P. *J. Mater. Chem.* **2004**, *14*, 3481.
(17) Roucoux, A.; Schulz, J.; Patin, H. *Chem. Rev.* **2002**, *102*, 3757.
(18) Hvolbæk, B.; Janssens, T. V. W.; Clausen, B. S.; Falsig, H.; Christensen, C. H.; Nørskov, J. K. *Nano Today* **2007**, *2*, 14.
(19) Li, Y.; Somorjai, G. A. *Nano Lett.* **2010**, *10*, 2289.

(20) Durand, J.; Teuma, E.; Gómez, M. *Eur. J. Inorg. Chem.* **2008**, *2008*, 3577.
(21) Crespo-Quesada, M.; Yarulin, A.; Jin, M.; Xia, Y.; Kiwi-Minsker, L. *J. Am. Chem. Soc.* **2011**, *133*, 12787.
(22) Zhou, X.; Xu, W.; Liu, G.; Panda, D.; Chen, P. *J. Am. Chem. Soc.* **2010**, *132*, 138.
(23) Wilson, O. M.; Knecht, M. R.; Garcia-Martinez, J. C.; Crooks, R. M. *J. Am. Chem. Soc.* **2006**, *128*, 4510.
(24) Jia, C.-J.; Schuth, F. *Phys. Chem. Chem. Phys.* **2011**, *13*, 2457.
(25) Somorjai, G. A.; Park, J. Y. *Angew. Chem., Int. Ed.* **2008**, *47*, 9212.
(26) Narayanan, R.; El-Sayed, M. A. *J. Am. Chem. Soc.* **2003**, *125*, 8340.
(27) Li, Y.; El-Sayed, M. A. *J. Phys. Chem. B* **2001**, *105*, 8938.
(28) Ma, L.; Abney, C.; Lin, W. *Chem. Soc. Rev.* **2009**, *38*, 1248.
(29) Chauhan, B. P. S.; Rathore, J. S.; Bandoo, T. *J. Am. Chem. Soc.* **2004**, *126*, 8493.
(30) Ooe, M.; Murata, M.; Mizugaki, T.; Ebitani, K.; Kaneda, K. *Nano Lett.* **2002**, *2*, 999.
(31) Tsuji, Y.; Fujihara, T. *Inorg. Chem.* **2007**, *46*, 1895.
(32) Crooks, R. M.; Zhao, M.; Sun, L.; Chechik, V.; Yeung, L. K. *Acc. Chem. Res.* **2001**, *34*, 181.
(33) Jiang, Y.; Gao, Q. *J. Am. Chem. Soc.* **2006**, *128*, 716.
(34) Ma, R.; Semagina, N. *J. Phys. Chem. C* **2010**, *114*, 15417.
(35) Alkilany, A. M.; Murphy, C. J. *Langmuir* **2009**, *25*, 13874.
(36) Cliffel, D. E.; Zamborini, F. P.; Gross, S. M.; Murray, R. W. *Langmuir* **2000**, *16*, 9699.
(37) Şen, F.; Gökağaç, G. *J. Phys. Chem. C* **2007**, *111*, 1467.
(38) Lu, F.; Ruiz, J.; Astruc, D. *Tetrahedron Lett.* **2004**, *45*, 9443.
(39) Zamborini, F. P.; Gross, S. M.; Murray, R. W. *Langmuir* **2001**, *17*, 481.
(40) Eklund, S. E.; Cliffel, D. E. *Langmuir* **2004**, *20*, 6012.
(41) Castro, E. G.; Salvatierra, R. V.; Schreiner, W. H.; Oliveira, M. M.; Zarbin, A. J. G. *Chem. Mater.* **2010**, *22*, 360.
(42) Li, Z.; Gao, J.; Xing, X.; Wu, S.; Shuang, S.; Dong, C.; Paau, M. C.; Choi, M. M. F. *J. Phys. Chem. C* **2010**, *114*, 723.
(43) Alvarez, J.; Liu, J.; Roman, E.; Kaifer, A. E. *Chem. Commun.* **2000**, 1151.
(44) Niu, Y.; Yeung, L. K.; Crooks, R. M. *J. Am. Chem. Soc.* **2001**, *123*, 6840.
(45) Oh, S.-K.; Niu, Y.; Crooks, R. M. *Langmuir* **2005**, *21*, 10209.
(46) Yeung, L. K.; Crooks, R. M. *Nano Lett.* **2001**, *1*, 14.
(47) Garcia-Martinez, J. C.; Lezutekong, R.; Crooks, R. M. *J. Am. Chem. Soc.* **2005**, *127*, 5097.
(48) Chechik, V.; Crooks, R. M. *J. Am. Chem. Soc.* **2000**, *122*, 1243.
(49) Narayanan, R.; El-Sayed, M. A. *J. Catal.* **2005**, *234*, 348.
(50) Mandal, S.; Roy, D.; Chaudhari, R. V.; Sastry, M. *Chem. Mater.* **2004**, *16*, 3714.
(51) Shon, Y.-S.; Chuc, S.; Voundi, P. *Colloid Surf. A* **2009**, *352*, 12.
(52) Brust, M.; Walker, M.; Bethell, D.; Schiffrin, D. J.; Whyman, R. *J. Chem. Soc., Chem. Commun.* **1994**, 801.
(53) Sardar, R.; Funston, A. M.; Mulvaney, P.; Murray, R. W. *Langmuir* **2009**, *25*, 13840.
(54) Parker, J. F.; Fields-Zinna, C. A.; Murray, R. W. *Acc. Chem. Res.* **2010**, *43*, 1289.
(55) Cargnello, M.; Wieder, N. L.; Canton, P.; Montini, T.; Giambastiani, G.; Benedetti, A.; Gorte, R. J.; Fornasiero, P. *Chem. Mater.* **2011**, *23*, 3961.
(56) Yee, C.; Scotti, M.; Ulman, A.; White, H.; Rafailovich, M.; Sokolov, J. *Langmuir* **1999**, *15*, 4314.
(57) Ibañez, F. J.; Zamborini, F. P. *Langmuir* **2006**, *22*, 9789.
(58) Sadeghmoghaddam, E.; Lam, C.; Choi, D.; Shon, Y.-S. *J. Mater. Chem.* **2011**, *21*, 307.
(59) Sadeghmoghaddam, E.; Gaïeb, K.; Shon, Y.-S. *Appl. Catal., A* **2011**, *405*, 137.
(60) Bhattacharjee, S.; Dotzauer, D. M.; Bruening, M. L. *J. Am. Chem. Soc.* **2009**, *131*, 3601.
(61) Miao, S.; Zhang, C.; Liu, Z.; Han, B.; Xie, Y.; Ding, S.; Yang, Z. *J. Phys. Chem. C* **2008**, *112*, 774.
(62) Wu, H.; Wu, C.; He, Q.; Liao, X.; Shi, B. *Mater. Sci. Eng., C* **2010**, *30*, 770.
(63) Ornelas, C.; Aranzaes, J. R.; Salmon, L.; Astruc, D. *Chem.—Eur. J.* **2008**, *14*, 50.
(64) Ornelas, C.; Ruiz, J.; Salmon, L.; Astruc, D. *Adv. Synth. Catal.* **2008**, *350*, 837.
(65) Huang, X.; Wang, Y.; He, Q.; Liao, X.; Shi, B. *Catal. Lett.* **2009**, *133*, 192.
(66) Jiang, Y.; Jiang, J.; Gao, Q.; Ruan, M.; Yu, H.; Qi, L. *Nanotechnology* **2008**, *19*, 075714.
(67) Wang, Y.; Lee, J.-K. *J. Mol. Catal. A: Chem.* **2007**, *263*, 163.
(68) Polshettiwar, V.; Luque, R.; Fihri, A.; Zhu, H.; Bouhrara, M.; Basset, J.-M. *Chem. Rev.* **2011**, *111*, 3036.
(69) Cadierno, V.; García-Garrido, S. E.; Gimeno, J.; Varela-Álvarez, A.; Sordo, J. A. *J. Am. Chem. Soc.* **2006**, *128*, 1360.
(70) van der Drift, R. C.; Bouwman, E.; Drent, E. *J. Organomet. Chem.* **2002**, *650*, 1.
(71) Uma, R.; Crévisy, C.; Grée, R. *Chem. Rev.* **2003**, *103*, 27.
(72) Sabitha, G.; Nayak, S.; Bhikshapathi, M.; Yadav, J. S. *Org. Lett.* **2011**, *13*, 382.
(73) Ito, M.; Kitahara, S.; Ikariya, T. *J. Am. Chem. Soc.* **2005**, *127*, 6172.
(74) Leung, D. H.; Bergman, R. G.; Raymond, K. N. *J. Am. Chem. Soc.* **2007**, *129*, 2746.
(75) Musolino, M. G.; De Maio, P.; Donato, A.; Pietropaolo, R. *J. Mol. Catal. A: Chem.* **2004**, *208*, 219.
(76) Zharmagambetova, A. K.; Ergozhin, E. E.; Sheludyakov, Y. L.; Mukhamedzhanova, S. G.; Kurmanbayeva, I. A.; Selenova, B. A.; Utkelov, B. A. *J. Mol. Catal. A: Chem.* **2001**, *177*, 165.
(77) Ibañez, F. J.; Zamborini, F. P. *J. Am. Chem. Soc.* **2008**, *130*, 622.
(78) Moreno, M.; Ibañez, F. J.; Jasinski, J. B.; Zamborini, F. P. *J. Am. Chem. Soc.* **2011**, *133*, 4389.
(79) Leff, D. V.; Brandt, L.; Heath, J. R. *Langmuir* **1996**, *12*, 4723.
(80) Bhattacharjee, S.; Bruening, M. L. *Langmuir* **2008**, *24*, 2916.
(81) Hostetler, M. J.; Wingate, J. E.; Zhong, C.-J.; Harris, J. E.; Vachet, R. W.; Clark, M. R.; Londono, J. D.; Green, S. J.; Stokes, J. J.; Wignall, G. D.; Glish, G. L.; Porter, M. D.; Evans, N. D.; Murray, R. W. *Langmuir* **1998**, *14*, 17.
(82) Hostetler, M. J.; Templeton, A. C.; Murray, R. W. *Langmuir* **1999**, *15*, 3782.
(83) Zhao, Z.; Sevryugina, Y.; Carpenter, M. A.; Welch, D.; Xia, H. *Anal. Chem.* **2004**, *76*, 6321.
(84) Sun, Y.; Tao, Z.; Chen, J.; Herricks, T.; Xia, Y. *J. Am. Chem. Soc.* **2004**, *126*, 5940.
(85) Musolino, M. G.; Cutrupi, C. M. S.; Donato, A.; Pietropaolo, D.; Pietropaolo, R. *Appl. Catal., A* **2003**, *243*, 333.
(86) Kidambi, S.; Bruening, M. L. *Chem. Mater.* **2005**, *17*, 301.
(87) Kidambi, S.; Dai, J.; Li, J.; Bruening, M. L. *J. Am. Chem. Soc.* **2004**, *126*, 2658.
(88) Scott, R. W. J.; Datye, A. K.; Crooks, R. M. *J. Am. Chem. Soc.* **2003**, *125*, 3708.
(89) Chen, X.; Wang, H.; He, J.; Cao, Y.; Cui, Z.; Liang, M. *J. Nanosci. Nanotechnol.* **2010**, *10*, 3138.
(90) Calver, C. F.; Dash, P.; Scott, R. W. J. *ChemCatChem* **2011**, *3*, 695.